J. Mol. Chem., 2024, 4(2), 693 Article

JOURNAL OF MOLECULAR CHEMISTRY

Computational molecular docking analysis of Doxifluridine and its metabolites to identify potential hits for PDHK1

Neeta Azad,[1,2] Rita Kakkar[1*]

[1]Computational Chemistry Group, Department of Chemistry, University of Delhi, Delhi-110007, India. [2]Department of Chemistry, Atma Ram Sanatan Dharam College, University of Delhi, Dhaula Kuan, New Delhi-110021, India

Submitted on: 25-Jan-2024, Accepted and published on: 15-Apr-2024

ABSTRACT

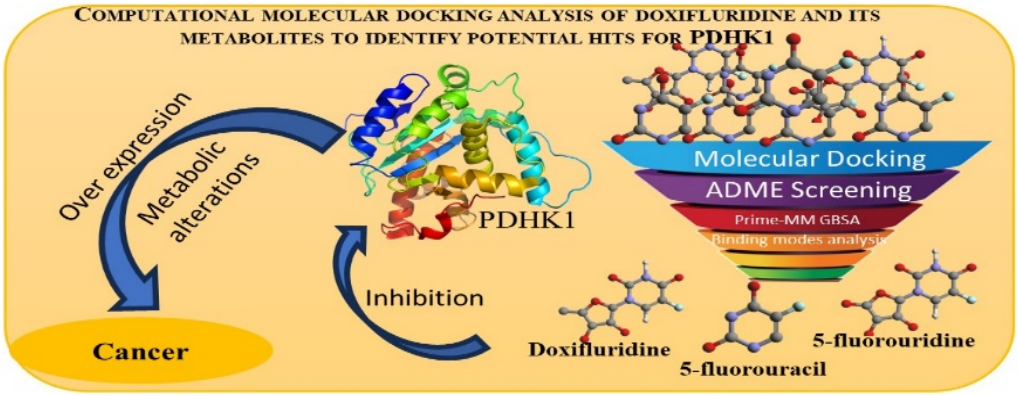

The development of targeted therapies for cancer and metabolic diseases remains a critical research area. The discovery of strong inhibitors of Pyruvate Dehydrogenase Kinase 1 (PDHK1), an enzyme essential for metabolic reprogramming, has been the focus of research in recent years. Doxifluridine, a prodrug of 5-fluorouracil, has shown promise for various cancer treatments. Additionally, its metabolites are of interest because of their potential medicinal effects. This paper presents a comprehensive computational molecular docking and dynamics analysis aimed at investigating the binding capabilities of doxifluridine and its metabolites as PDHK1 inhibitors. Molecular docking analysis revealed that doxifluridine and its metabolites displayed favorable binding interactions within the ATP-binding pocket of PDHK1, with docking scores of -11.84, -6.39, and -11.35 kcal/mol for doxifluridine, 5-fluorouracil, and 5-fluororouridine, respectively. The binding energies of these ligands (-37.32, -20.90, and -28.19 kcal/mol, respectively) suggest their potential inhibitory activity against PDHK1. Furthermore, specific amino acid residues involved in ligand binding have been identified, elucidating the key interactions required for stabilization. Molecular dynamics simulations reveal that these interactions are retained throughout a simulation period of 100 ns and the binding energy is -57.83±3.40 kcal/mol.

Keywords: Doxifluridine, PDHK1, 5-fluorouracil, 5-fluorouridine, molecular docking, Cancer drugs,

INTRODUCTION

Metabolic reprogramming is a hallmark of various diseases including cancer. The pyruvate dehydrogenase kinase family, including PDHK1, has garnered attention as a promising therapeutic target because of its role in the regulation of glucose metabolism.[1] Phosphorylation of the pyruvate dehydrogenase complex (PDC) by PDHK1 hinders the conversion of pyruvate to acetyl-CoA, resulting in increased glycolytic flux and lactate generation. Inhibition of PDHK1 can restore PDC activity and shift cellular metabolism from glycolysis to oxidative phosphorylation, ultimately inhibiting cancer cell proliferation and tumor growth.

PDHK1 inhibitors have gained interest as potential therapeutic agents for various diseases including cancer, diabetes, and metabolic disorders.[1,2] These compounds promote the activity of PDC by inhibiting PDHK1, which can enhance glucose oxidation and shift cellular metabolism to increased energy production.[3] PDHK1 inhibitors have been investigated as potential anticancer agents because of their ability to disrupt the Warburg effect, a metabolic adaptation characterized by increased glycolysis and reduced mitochondrial respiration observed in many cancer cells.[4–8]

*Corresponding Author: Prof. Rita Kakkar
Email: rkakkar@chemistry.du.ac.in

Doxifluridine is an antimetabolite prodrug of 5-fluorouracil (5-FU), commonly referred to as 5'-deoxy-5-fluorouridine (5'-DFUR). It is used as an oral prodrug of 5-FU in the treatment of various cancers, including gastric, colorectal, and breast cancer[9]. 5'-DFUR is converted to 5-FU by thymidine phosphorylase (TP) in tumor tissues (Scheme 1), leading to the inhibition of DNA synthesis and cell proliferation.[10,11]

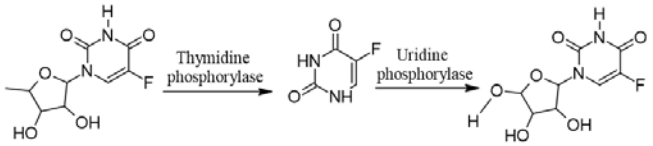

Scheme 1: Conversion of doxifluridine to 5-FU by thymidine phosphorylas

5-FU is quickly digested by the body, especially in the liver, where it produces a number of metabolites with well-known anticancer activities.[12] Following 5-FU metabolism, uridine phosphorylase removes it from the plasma and converts it to 5-fluorouridine (5-FUrd) (Scheme 1). The rate-limiting step of this process is this conversion.[13]

Although 5-FU and 5-FUrd have anticancer properties, doxifluridine is not immediately cytotoxic.[9,14] Iyer et al. conducted a concurrent pharmacokinetic investigation of doxifluridine, 5-FU, and 5-FUrd, and discovered the significance of the doxifluridine dosing regimen.[15] Thymidine phosphorylase activity, which is expressed at a higher level in tumor tissues than in normal tissues,[16,17] is associated with the selective anticancer action of 5'-DFUR.[18] Although 5-FU's effectiveness in treating tumors is well known,[19] resistance to the drug is regularly observed and continues to be its main drawback. Even when tumor cells were resistant to 5-FU, doxifluridine still exhibited anticancer efficacy.[20]

The cytotoxicity of 5'-DFUR on human bone marrow stem cells and human tumor cell lines was experimentally investigated, and the results supported the cytotoxicity of the drug against human tumor cells.[21] Additionally, a comparison of 5'-DFUR and 5-FU confirmed that 5'-DFUR has a higher therapeutic index.[22] The relationship between doxifluridine and PDHK1 inhibition may not have been extensively studied, but there may be some evidence to suggest a connection between these two areas. Since doxifluridine is metabolized to 5-FU, an antimetabolite, there could be potential implications for cellular metabolism, including alterations in glucose metabolism and mitochondrial function.[23] Some studies have explored the effects of 5-FU on PDHK1 and its potential as a PDHK1 inhibitor.[24]

In the present study, we computationally tested doxifluridine and its two metabolites (5-fluorouracil and 5-fluorouridine) as PDHK1 inhibitors. A docking method was used for this purpose. The ADME properties of the three compounds were calculated and analyzed to determine the factors responsible for the cytotoxic effects of doxifluridine. Molecular dynamics (MD) studies were used to validate the docking data.

METHODOLOGY

In this study, we employed computational tools to investigate the interaction of doxifluridine and its metabolites with PDHK1. The protein structure of PDHK1 [PDB ID: *2Q8G*] was obtained from the Protein Data Bank (*www.rcsb.org*), while doxifluridine and its metabolites were sketched, and their energy was minimized using the MacroModel program of Schrödinger with the OPLS-2005 force field.[25] Molecular docking simulations were performed using the state-of-the-art algorithm Glide-XP (Glide "extra precision") to predict the binding affinity and mode of interaction.[26–28]

The compound library for this work comprised three molecules: doxifluridine, 5-fluorouracil, and 5-fluorouridine. Each ligand structure was assigned an appropriate bond order and ionization state at physiological pH (7 ± 2) using the LigPrep module of Schrödinger, Inc.

Along with ligand refinement, LigPrep also generates stereoisomers. There are four chiral centers in both doxifluridine and 5-fluorouracil and no chiral center in 5-fluorouracil. Therefore, 33 structures were obtained as a result of the ligand preparation. These include 16 stereoisomers of doxifluridine, one of 5-fluorouracil (Scheme 2), and 16 stereoisomers of 5-fluorouridine. These 33 ligands (Table S1, SI) were docked into the prepared protein PDHK1 structure, and the results were analyzed. Further details of the computations are provided in Supporting Information (SI).

The stability of the binding mode of doxifluridine was examined by running MD simulations using Desmond simulation software[29,30] from Schrödinger, LLC. The model employed was an explicit solvent containing TIP3P water molecules[31]. Three Cl^- ions were introduced into the mixture to balance the charge. The system was supplemented with a 0.15 M NaCl solution to replicate the physiological environment. Further details are provided in the Supporting Information and in our earlier work.[32]

RESULTS AND DISCUSSION

BINDING MODE OF DOXIFLURIDINE

To study and understand the binding of various doxifluridine states to the PDHK1 active site, these states were docked into the protein-binding site. The pdb file *2Q8G* contains PDHK1 complexed with its known inhibitor AZD7545.[33] To obtain the protein structure, QM/MM treated ligand AZD7545 was first removed from the protein and re-docked. It docked at the same binding site with a Glide score of -11.53 kcal mol^{-1}.

An important feature of the binding cavity is its hydrophobic nature. Most drug binding to proteins is based on the fact that they possess hydrophobic groups. The same pattern was observed for PDHK1-AZD7545 binding. Hydrophobic (orange surfaces) and hydrophilic (light blue surfaces) maps were generated for the PDHK1 protein to see the nature of its binding cavity. The ligand is fully entrenched in the hydrophobic portion of the cavity (Figure 1). This indicates that the hydrophobic region of the protein plays a role in both the strong binding of the ligand and its inhibition. The 16 doxifluridine states docked to the same binding site. The analysis of the Glide-XP data, given in Table 1, shows that state D1 has the highest GlideScore, -11.84 kcal/mol).

This value is higher than that (-11.53 kcal mol^{-1}) for the original ligand, AZD7545. Apart from the GlideScore, E_{model} is also best for the D1 pose of doxifluridine, which adds to its favorable binding with the protein. This is because the functional groups are arranged in a manner that makes the most positive interactions with the protein. A visual representation of doxifluridine D1 binding to the active site is shown in Figure 2. The ligand is represented in the ball-and-stick model, and the protein is shown in ribbon form for the sake of clarity.

Figure 3 shows the ligand interaction diagram for D1. There are two hydrogen bonds between Ser75…OH, one Gln61…NH hydrogen bond, one π-π stacking with Phe78, and two water-mediated hydrogen bonds of C=O with Phe62 and Gln197. There are 12 water molecules inside the binding cavity of PDHK1, which facilitate hydrogen bonding with the polar groups of the ligands through water bridges during docking.

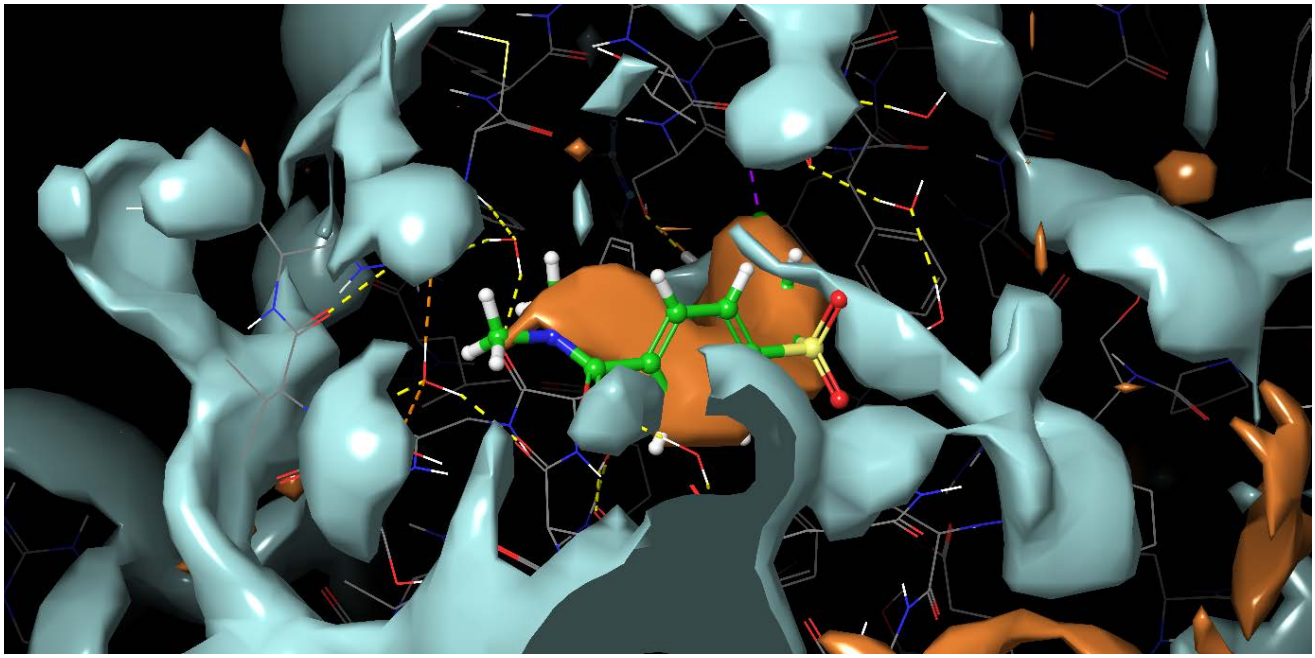

Figure 1 Hydrophobic and hydrophilic maps of the protein cavity holding the ligand in its hydrophobic part

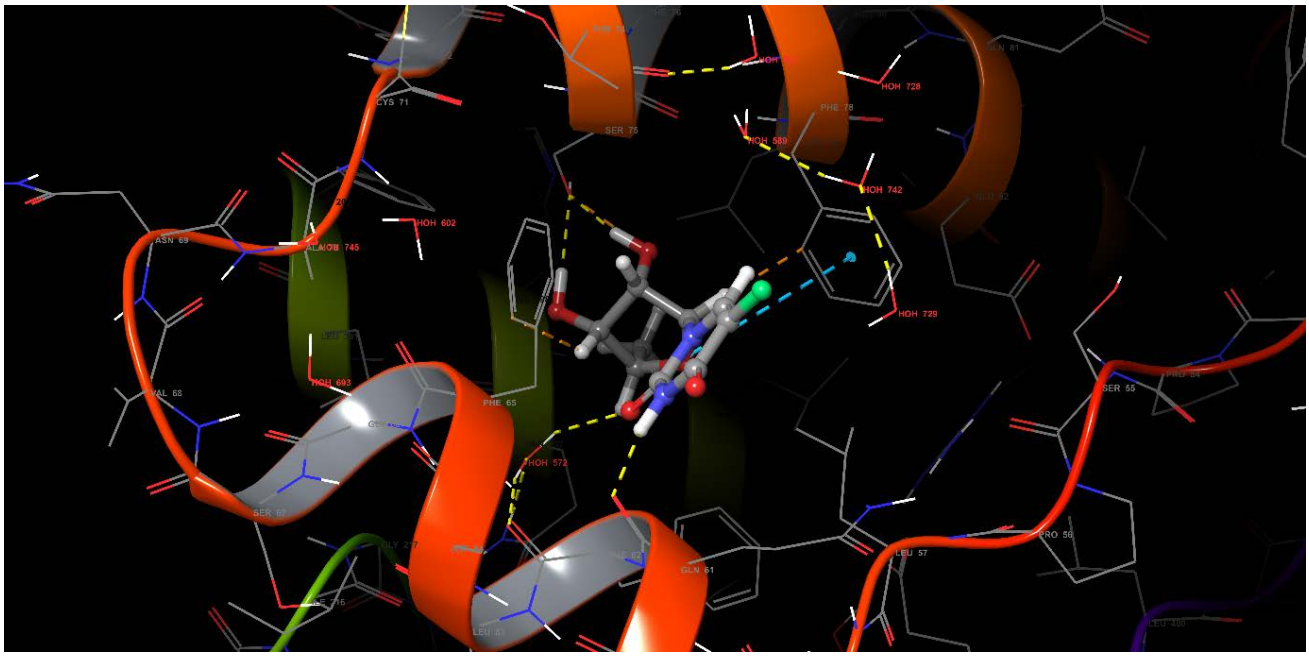

Figure 1 D1 complexed with PDHK1.

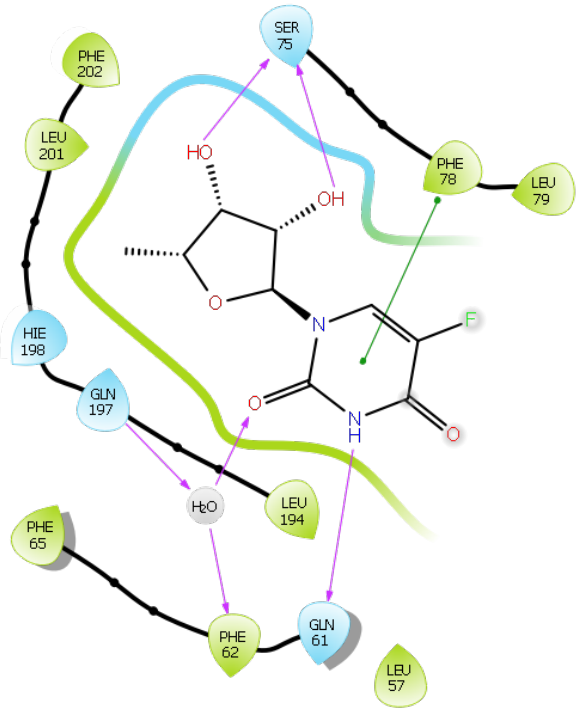

Figure 3 Ligand interaction diagram for D1. Residues colored green are hydrophobic and those colored blue are polar.

Table 1 Glide-XP data (kcal/mol) for doxifluridine states and 5-FU

Title	Glide score	E_{vdW}	E_{coul}	Glide energy	$E_{internal}$	E_{model}	HBond
D1	-11.84	-24.97	-13.38	-38.35	3.94	-60.61	-2.52
D2	-11.45	-31.06	-9.22	-40.28	3.22	-53.93	-2.48
D3	-10.32	-28.62	-4.60	-33.22	1.96	-48.46	-1.75
D4	-9.90	-33.92	-3.86	-37.78	3.16	-49.25	-1.65
D5	-9.64	-33.03	-4.47	-37.50	5.52	-44.06	-0.96
D6	-9.48	-29.78	-5.33	-35.11	2.76	-41.80	-1.06
D7	-9.48	-29.05	-6.21	-35.26	6.82	-50.94	-1.44
D8	-9.20	-33.25	-5.97	-39.22	3.26	-55.66	-2.42
D9	-8.83	-28.54	-11.57	-40.11	7.43	-57.43	-2.06
D10	-8.49	-28.32	-8.66	-36.97	3.16	-47.76	-2.10
D11	-8.24	-28.20	-4.41	-32.62	1.81	-48.72	-1.37
D12	-7.87	-22.84	-8.36	-31.20	10.87	-43.14	-1.92
D13	-7.85	-24.00	-6.25	-30.25	0.80	-39.26	-1.66
D14	-7.28	-26.28	-5.58	-31.86	1.52	-47.33	-1.75
D15	-7.27	-35.29	0.63	-34.66	0.84	-41.87	-0.96
D16	-5.92	-31.67	-1.52	-33.18	7.51	-43.13	-0.90
5-FU	-6.39	-19.24	-4.77	-24.01	0.00	-31.76	-1.04

Prime MM/GBSA Gibbs energies of binding

The Gibbs energy of binding ΔG^1_{bind} corresponds to the forward inhibition reaction:

receptor + ligand → receptor-ligand (1)

A more negative value of the Gibbs energy of binding indicates greater favorability of this inhibition reaction. We proceeded in the same manner as in our previous studies on PDHK2 inhibitors[34–36]. The ΔG^1_{bind} values for the 16 poses of doxifluridine are tabulated in Table 2, which also lists their ΔG^2_{bind} values. ΔG^1_{bind} refers to the Gibbs binding energy with the ligand strain energy included, and ΔG^2_{bind} refers to the Gibbs binding energy without ligand strain. When an otherwise free ligand is complexed with the receptor, strain is induced in the ligand. As a result, the Gibbs energy of binding must also consider the ligand strain energies; hence, we examined the data using the ΔG^1_{bind} values.

The Gibbs energy of binding ΔG^1_{bind} and strain energy are interrelated. The smaller the strain energy, the less the ligand will have to distort itself in order to bind to the receptor; thus, the forward inhibition reaction is more favorable. From our Prime MM/GBSA calculations, we obtained the strain energy of each ligand. These values are listed in Table 2, and were calculated using Equation (2).

Table 2 Prime MM/GBSA Gibbs binding energies (kcal/mol) for Doxifluridine states

Title	ΔG^1_{bind}	ΔG^2_{bind}	L_{Strain}
D1	-37.32	-38.40	1.08
D2	-31.56	-34.89	3.33
D3	-25.56	-27.95	2.39
D4	-24.34	-26.82	2.48
D5	-15.38	-20.23	4.85
D6	-19.95	-22.87	2.91
D7	-28.58	-35.49	6.91
D8	-22.72	-26.36	3.64
D9	-23.52	-33.77	10.25
D10	-25.38	-32.56	7.18
D11	-12.28	-21.37	9.09
D12	-33.11	-34.17	1.06
D13	0.29	-15.13	15.42
D14	-16.87	-25.01	8.14
D15	-16.34	-20.73	4.39
D16	-19.62	-25.95	6.32

$$L_{strain\_energy} = L_{energy\_within\_complex} - L_{free} \quad (2)$$

where $L_{energy\_within\_complex}$ is the Prime MM/GBSA energy of the ligand within the receptor-ligand complex, L_{free} is the Prime MM/GBSA energy of the free ligand, and L_{strain_energy} is the strain energy of the ligand upon complexation. Therefore, the Gibbs energy of binding, including the ligand strain (ΔG^1_{bind}), can be calculated from the following equation:

$$\Delta G^1_{bind} = \Delta G^2_{bind} + L_{strain\_energy} \quad (3)$$

It is noteworthy that the state D1 of doxifluridine has the most negative value of ΔG^1_{bind} and one of the smallest values of strain energy (Table 2), indicating that this state is the most favorable and that the ligand in this configuration is already in a suitable form for binding. The ADME properties and descriptors of this compound are listed in Tables S2 and S3 (SI). All properties fall within the recommended range of 95% of known drugs. No violations of Lipinski's Rule of Five were observed.

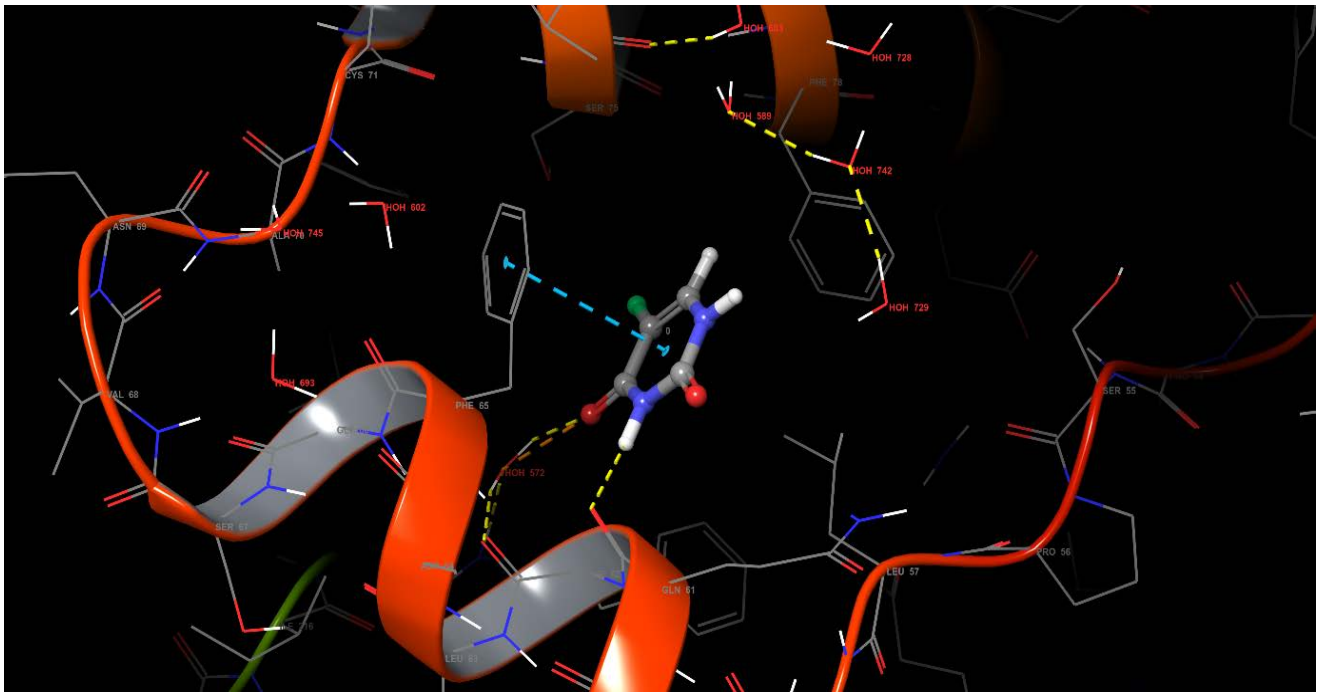

Figure 4 Docked form of 5-fluorouracil in the binding cavity of PDHK1. The ligand forms a Gln61…H-N hydrogen bond, a water mediated hydrogen bond with Phe62, and a π-π stacking interaction with Phe65

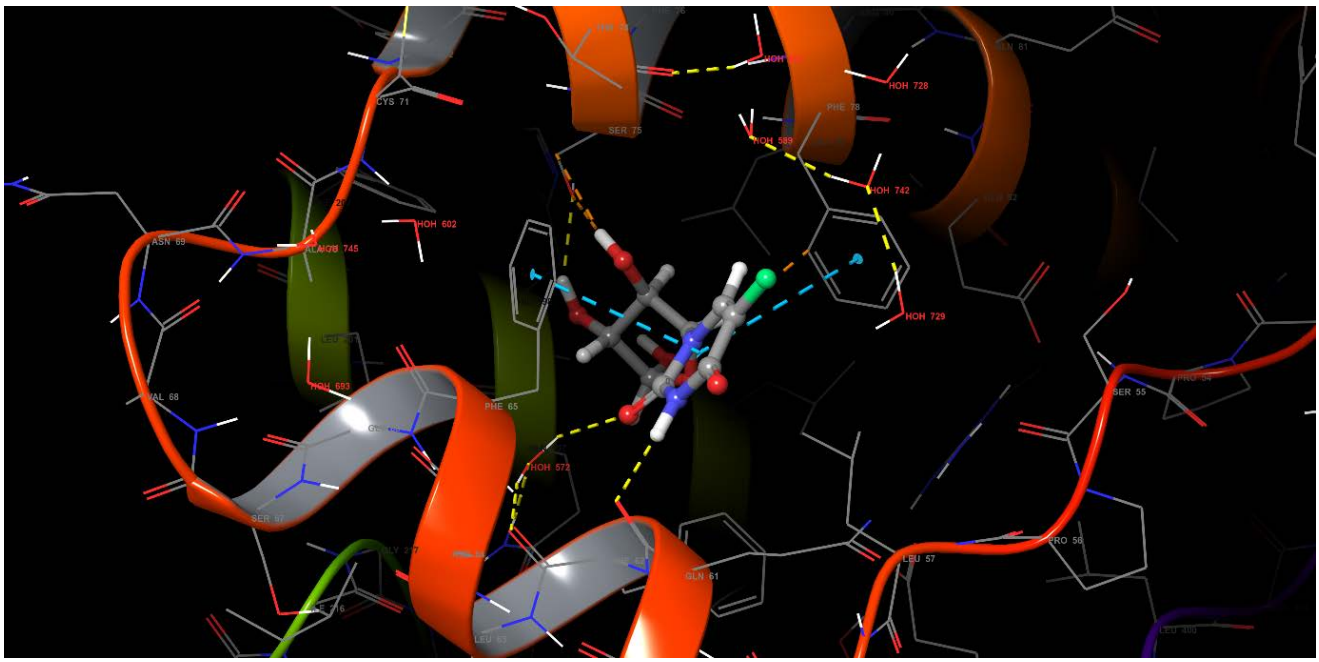

Figure 2 Complex form of PDHK1 with ligand U1.

Binding mode of 5-fluorouracil

5-fluorouracil is one of the metabolites obtained from doxifluridine in the presence of thymidine phosphorylase. To test the binding and inhibition possibilities of 5-fluorouracil, it was docked into the PDHK1 protein. The results are presented in Table 1. The docking score is acceptable but not as good as that for doxifluridine. A possible reason for this may be the smaller size of the molecule. The cavity of PDHK1 is much larger than the ligand. Although it is completely embedded in the hydrophobic cavity, the ligand cannot engage all residues responsible for binding to the pyruvate dehydrogenase complex unit. 5-fluorouracil forms only one hydrogen bond with its receptor. The residue Gln61 forms a hydrogen bond with the hydrogen of the -NH group, and another water-mediated

hydrogen bond is formed between Phe62 and one of the carbonyl oxygens of the ligand (Figure 4). Hydrophobic π–π stacking interactions with Phe62 were also observed.

The Prime MM/GBSA Gibbs binding energy for 5-fluorouracil is acceptable (ΔG^1_{bind} = -20.90 kcal mol^{-1}; ΔG^2_{bind} = -21.04 kcal mol^{-1}), but much smaller than the Gibbs free energies for doxifluridine (Table 2). The ligand strain energy is very low (0.14 kcal mol^{-1}).

The ADME properties and descriptors of the compound were also calculated. The values of these properties are listed in Tables S4 and S5 (SI). All predicted properties lie within the recommended range, except for polrz and logPC16. No violations of Lipinski's rules were observed.

Binding mode of 5-fluorouridine

5-fluorouridine was also tested for its inhibition of PDHK1. Before that, its various states were generated, as described earlier. The best pose obtained after docking was U1, which showed the best Glide Score (Table 3). This score is comparable to that of doxifluridine, because both structures have functional group similarities. Its E_{model} value was also the best among the obtained values for various states of 5-fluorouridine. All the other parameters, E_{vdW}, E_{coul}, $E_{internal}$, and Glide energy, were again the best on their scale for the U1 state. This suggests that this state of 5-fluorouridine fits the PDHK1 binding cavity in the best manner. The other state that competes with U1 based on its Glide parameters is U9.

Table 3 Glide-XP data (kcal/mol) for 5-fluorouridine states

Title	Glide Score	E_{vdW}	E_{coul}	Glide energy	$E_{internal}$	E_{model}	HBond
U1	-11.35	-34.99	-9.63	-44.63	5.20	-58.59	-3.10
U2	-11.28	-34.11	-8.12	-42.23	1.51	-55.45	-3.02
U3	-11.25	-29.09	-11.23	-40.32	3.39	-53.56	-2.26
U4	-11.21	-34.24	-9.42	-43.67	4.98	-65.43	-1.96
U5	-11.07	-34.29	-9.73	-44.01	6.61	-51.65	-2.84
U6	-10.39	-31.25	-5.88	-37.13	2.56	-55.11	-1.75
U7	-8.89	-26.92	-9.10	-36.01	7.66	-48.31	-2.13
U8	-8.87	-31.74	-7.24	-38.98	3.29	-57.96	-1.80
U9	-8.69	-29.20	-12.35	-41.55	4.19	-61.03	-2.37
U10	-8.37	-30.94	-9.81	-40.75	6.21	-56.35	-2.40
U11	-8.13	-27.84	-6.61	-34.45	7.15	-44.94	-2.19
U12	-8.12	-30.03	-7.64	-37.68	0.94	-48.62	-1.86
U13	-8.11	-28.39	-8.06	-36.45	3.29	-53.72	-1.95
U14	-7.99	-26.14	-8.33	-34.47	10.49	-47.83	-2.48
U15	-7.74	-30.18	-4.70	-34.88	1.95	-50.32	-1.29
U16	-7.44	-35.56	-6.47	-42.02	4.85	-60.74	-1.69

Based on a close examination of the docked form of U1, we concluded that the position of the ligand in the protein cavity was almost the same. The six- and five-membered rings were positioned in the same place. The only difference was the orientation of the functional groups. The same residues of the protein are responsible for the formation of hydrogen bonds between the receptor and the ligand. Figure 5 shows a pictorial representation of U1 in the binding cavity of the protein PDHK1. The same observation was made for the U1 ligand as for doxifluridine. U1 is also present in the orange region of the protein, almost at the same position. The orientation of the ligand is also similar, and hydrogen bond formation between the ligand and receptor also occurs between the same residues (Figure 6), with the exception of an additional π-π stacking interaction with Phe65.

Gibbs binding energy calculations were performed on the U-FUrd states to know how easily they fit into the binding cavities in the protein. The Gibbs binding energies ΔG^1_{bind}, ΔG^2_{bind}, and ligand strain energies were the smallest for the U8 state of 5-fluorouridine (Table 4). The U1 state shows a good value for ΔG^1_{bind}, but the ligand strain energy is high for this state, which implies that U1 requires more effort to fit into the cavity than U8 does.

Tables S6 and S7 (SI) show ADME and other properties of this ligand. They all fall within the range of 95% of known drugs, indicating that it is druggable.

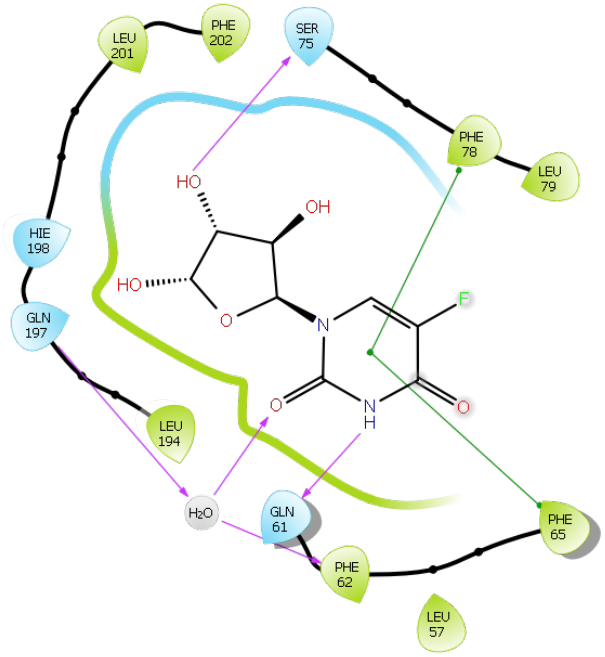

Figure 6 Ligand interaction diagram for U1

Table 4: Prime MM/GBSA Gibbs binding energy (kcal/mol) for 5-fluorouridine states

Title	ΔG^1_{bind}	ΔG^2_{bind}	L_{Strain}
U1	-28.19	-36.73	8.54
U2	-27.87	-33.72	5.86
U3	-25.25	-29.35	4.09
U4	-27.40	-32.73	5.33
U5	-27.70	-32.47	4.77
U6	-28.00	-30.12	2.11
U7	-15.19	-24.99	9.80
U8	-30.34	-30.63	0.29
U9	-19.43	-29.47	10.04
U10	-27.55	-30.61	3.06
U11	-18.34	-21.37	3.02
U12	-25.82	-26.61	0.79
U13	-26.13	-32.19	6.06
U14	-15.18	-23.54	8.36
U15	-27.28	-31.12	3.84
U16	-19.71	-29.37	9.66

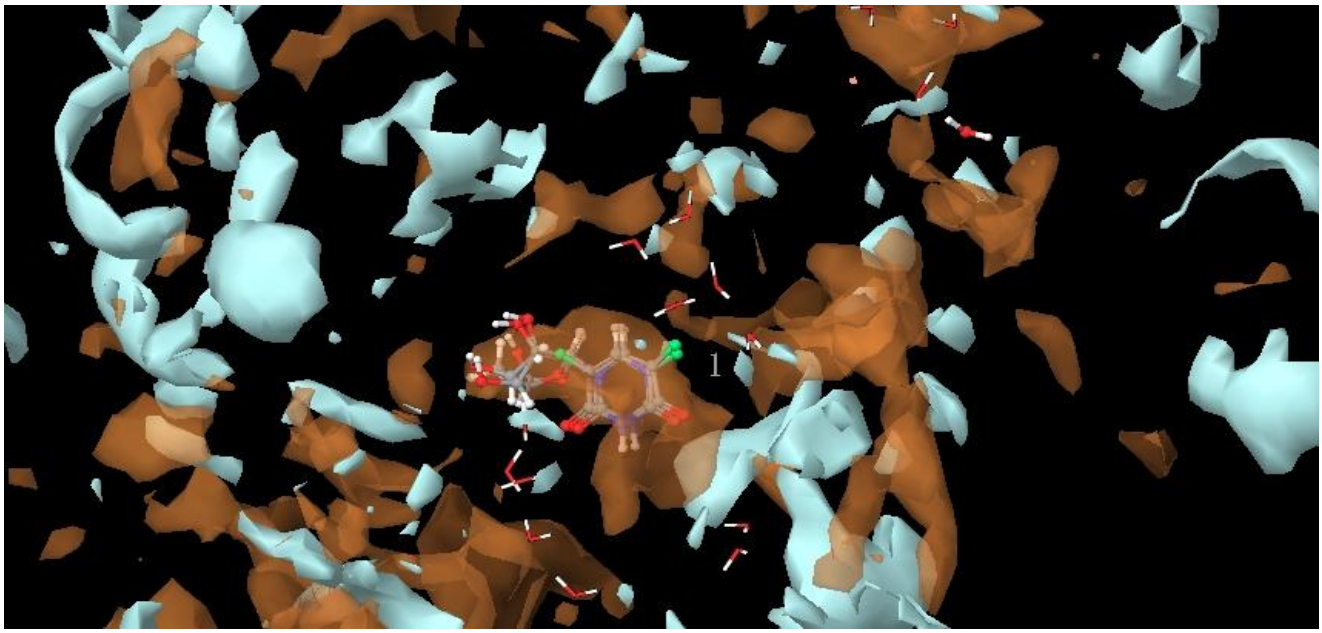

Figure 7 Overlapping of D1, U1, and 5-FU in the protein binding cavity

Comparison of binding of doxifluridine, 5-fluorouracil, and 5-fluorouridine to PDHK1

To determine the exact position of the three ligands (D1, U1, and 5-FU), they were overlapped (Figure 7). Their positions were identical in the hydrophobic pocket, with the only difference being their orientation.

Table 5 Number of van der Waals contacts formed between the ligands and PDHK1

Ligand	Good contacts	Bad contacts	Ugly contacts
Doxifluridine (D1)	257	8	1
5-fluorouracil	239	4	0
5-fluorouridine (U1)	109	0	0

A detailed structural analysis based on the number of close contacts between the ligands and the protein PDHK1 gives an idea into the contribution of hydrogen bonding and van der Waals contacts to the stability of the complex formed. The results of the contact analysis are presented in Table 5. Depending on the contact cutoff ratio, the contacts can be divided into three categories: good, bad, and ugly. The contact cutoff ratio is ugly when it is < 0.75, bad when it is < 0.89, and good when it is < 1.3. For the PDHK1-D1 complex, the number of good contacts was the highest, but there were also many bad and ugly contacts. In the case of U1, bad and ugly contacts do not exist, and only favorable interactions occur for the complex PDHK1-U1.

However, a more detailed discussion of the stability of the binding modes cannot be made without explicit molecular dynamics calculations; hence, we subjected the best docking ligand D1 to a 100 ns molecular dynamics simulation.

Molecular Dynamics Simulations

The ligand-protein contacts for D1 are shown in Figure 8.

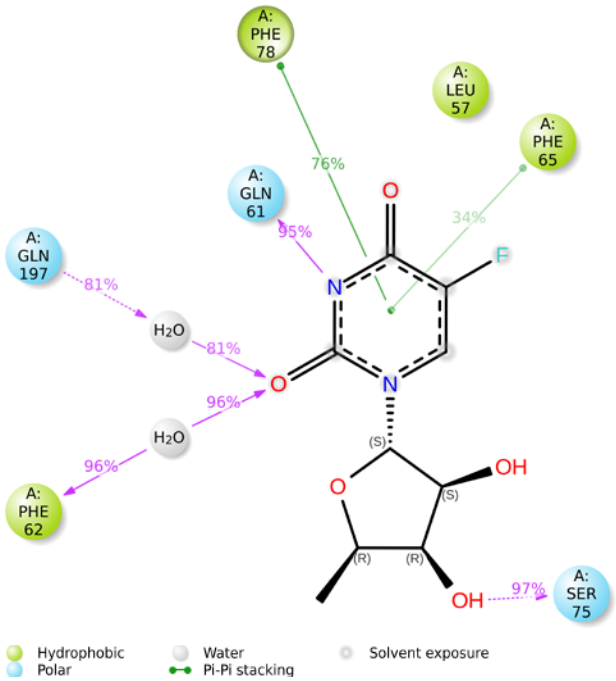

Figure 8 Ligand-protein contacts for D1-PDHK1

A comparison with Figure 3 reveals that nearly all interactions in the docked structure were conserved during the MD run. The exception was that Ser75 formed a hydrogen bond with only one OH group instead of both, and a new hydrophobic π-π stacking interaction with Phe65 was also present. This shows that the ligand makes several hydrogen bonds, hydrophobic, and water bridging contacts with the protein, which contributes to binding stability. The calculated MM-GBSA binding energy is -57.83±3.40 kcal mol^{-1}. This is higher than the computed value, -

37.32 kcal mol^{-1} (see Table 2), for the static structure, signifying increase in the interactions over time.

CONCLUSIONS

Doxifluridine and its metabolites (5-fluorouracil and 5-fluorouridine) have been found to act as anticancer agents for various cancer treatments. PDHK1 is also upregulated in cancer cells and needs to be regulated. Hence, various stereoisomers of doxifluridine, 5-fluorouracil, and 5-fluorouridine were tested computationally for their PHDK1 inhibiting capability. A total of 16 stereoisomers exist for doxifluridine and 5-fluorouridine, but only one form of 5-fluorouracil exists, owing to the lack of chiral centers. The 33 states of the three compounds were taken up for docking studies, and their most favorable forms were detected based on docking and Prime MM/GBSA calculations and their favorable and unfavorable interactions with the protein residues. The D1 state of doxifluridine fits the PDHK1 binding cavity better than the other forms. Similarly, the U1 state of 5-fluorouridine fits the protein in a better manner with no resistance contacts. Both D1 and U1 showed better docking scores than the original ligand AZD745 did. 5-fluorouracil has a lower Glide score and Gibbs binding energy. The docked structure for doxifluridine was stable over time, as revealed by MD studies.

FUTURE PERSPECTIVES

Computational molecular docking analysis is a valuable tool in the early stages of drug discovery[37]. This study sheds light on the potential of doxifluridine and its metabolites as PDHK1 inhibitors. Exploiting the therapeutic potential of these compounds may open new avenues for targeted cancer therapy and metabolic disease treatment. However, careful experimental validation is required to translate these findings into clinical application.

Fluorouracil resistance remains a significant obstacle in cancer treatment, necessitating the development of novel therapeutic approaches. PDHK1 inhibition has emerged as a promising strategy to sensitize tumor cells to 5-FU and overcome resistance. Preclinical evidence and early clinical trials have highlighted the potential of PDHK1 inhibitors as adjuvant therapies for enhancing the efficacy of 5-FU. Further research and extensive clinical studies are warranted to establish the safety and efficacy of PDHK1 inhibition in combination with 5-FU, as a potential therapeutic approach for cancer treatment. If successful, this innovative approach could bring us closer to improving patient outcomes and offer new hope for those facing drug-resistant malignancies.

Identification of favorable binding interactions within the ATP-binding pocket of PDHK1 suggests that doxifluridine and its metabolites have potential as effective inhibitors. This discovery not only underscores the importance of repurposing existing drugs for new therapeutic applications, but also highlights the significance of understanding molecular interactions at the atomic level in drug design.

Moreover, the elucidation of the specific amino acid residues involved in ligand binding provides invaluable information for further optimization of PDHK1 inhibitors. By delineating the key interactions required for stabilization, this study paves the way for the design and development of more potent and selective inhibitors, ultimately enhancing their efficacy in cancer and metabolic disease treatments.

The computational findings presented in this study provide valuable insights into the potential use of doxifluridine and its metabolites as PDHK1 inhibitors. However, further experimental validation, such as *in vitro* and *in vivo* studies, are essential to fully confirm their inhibitory activity and therapeutic potential. Moreover, structure-activity relationship (SAR) studies would be beneficial for designing and optimizing more potent PDHK1 inhibitors based on doxifluridine and its metabolites.

CONFLICT OF INTEREST STATEMENT

Authors declare that there is no academic or financial conflict of interest for this work.

REFERENCES AND NOTES

1. X. Wang, X. Shen, Y. Yan, H. Li. Pyruvate dehydrogenase kinases (PDKs): an overview toward clinical applications. *Biosci Rep* **2021**, 41 (4).
2. A. Ghinet, X. Thuru, E. Floquet, et al. Enhanced antitumor potential induced by chloroacetate-loaded benzophenones acting as fused tubulin-pyruvate dehydrogenase kinase 1 (PDHK1) ligands. *Bioorg Chem* **2020**, 96, 103643.
3. R. Pal, D. Hui, H. Menchen, et al. Protection against Aβ-induced neuronal damage by KU-32: PDHK1 inhibition as important target. *Front Aging Neurosci* **2023**, 15, 1282855.
4. L. Pinzi, F. Foschi, M.S. Christodoulou, D. Passarella, G. Rastelli. Design and Synthesis of Hsp90 Inhibitors with B- Raf and PDHK1 Multi-Target Activity. *ChemistryOpen* **2021**, 10 (12), 1177–1185.
5. N. Chatterjee, E. Pazarentzos, M.K. Mayekar, et al. Synthetic Essentiality of Metabolic Regulator PDHK1 in PTEN-Deficient Cells and Cancers. *Cell Rep* **2019**, 28 (9), 2317-2330.e8.
6. M. Yu, Q. Pan, W. Li, et al. Isoliquiritigenin inhibits gastric cancer growth through suppressing GLUT4 mediated glucose uptake and inducing PDHK1/PGC-1α mediated energy metabolic collapse. *Phytomedicine* **2023**, 121, 155045.
7. M. Kumari, B.S. Chhikara, P. Singh, B. Rathi, G. Singh. Signaling and molecular pathways implicated in oral cancer: A concise review. *Chem. Biol. Lett.* **2024**, 11 (1), 652.
8. B.S. Chhikara, K. Parang. Global Cancer Statistics 2022: the trends projection analysis. *Chem. Biol. Lett.* **2023**, 10 (1), 451.
9. J.M. Joulia, F. Pinguet, M. Ychou, et al. Pharmacokinetics of 5-fluorouracil (5-FUra) in patients with metastatic colorectal cancer receiving 5-FUra bolus plus continuous infusion with high dose folinic acid (LV5FU2). *Anticancer Res* **1997**, 17 (4A), 2727–2730.
10. W. Bollag, H.R. Hartmann. Tumor inhibitory effects of a new fluorouracil derivative: 5′-deoxy-5-fluorouridine. *European Journal of Cancer (1965)* **1980**, 16 (4), 427–432.
11. C. Sethy, C.N. Kundu. 5-Fluorouracil (5-FU) resistance and the new strategy to enhance the sensitivity against cancer: Implication of DNA repair inhibition. *Biomedicine & Pharmacotherapy* **2021**, 137, 111285.
12. H.M. Pinedo, G.F. Peters. Fluorouracil: biochemistry and pharmacology. *Journal of Clinical Oncology* **1988**, 6 (10), 1653–1664.
13. H. Ishitsuka, M. Miwa, K. Takemoto, et al. Role of uridine phosphorylase for antitumor activity of 5'-deoxy-5-fluorouridine. *Gan* **1980**, 71 (1), 112–123.
14. L.J. Schaaf, B.R. Dobbs, I.R. Edwards, D.G. Perrier. The pharmacokinetics of doxifluridine and 5-fluorouracil after single intravenous infusions of doxifluridine to patients with colorectal cancer. *Eur J Clin Pharmacol* **1988**, 34 (5), 439–443.
15. I. Baek, B. Lee, W. Kang, K. Kwon. Comparison of average, scaled average, and population bioequivalence methods for assessment of

highly variable drugs: an experience with doxifluridine in beagle dogs. *Eur J Pharm Sci* **2010**, 39 (1–3), 175–180.
16. N. Kobayashi, T. Kubota, M. Watanabe, et al. Pyrimidine nucleoside phosphorylase and dihydropyrimidine dehydrogenase indicate chemosensitivity of human colon cancer specimens to doxifluridine and 5-fluorouracil, respectively. *Journal of Infection and Chemotherapy* **1999**, 5 (3), 144–148.
17. S. Hiroyasu. Clinical Relevance of the Concentrations of Both Pyrimidine Nucleoside Phosphorylase (PyNPase) and Dihydropyrimidine Dehydrogenase (DPD) in Colorectal Cancer. *Jpn J Clin Oncol* **2001**, 31 (2), 65–68.
18. Y. Hata, H. Takahashi, F. Sasaki, et al. Intratumoral pyrimidine nucleoside phosphorylase (pynpase) activity predicts a selective effect of adjuvant 5'-deoxy-5-fluorouridine (5' dfur) on breast cancer. *Breast Cancer* **2000**, 7 (1), 37–41.
19. S. Kumar, A.K. Mishra, B.S. Chhikara, K. Chuttani, R.K. Sharma. Preparation and pharmacological evaluation of a new radiopharmaceutical, technetium-99m-5-fluorouracil, for tumor scintigraphy. *Hell J Nucl Med* **2008**, 11 (2), 91–95.
20. E. Bajetta, M. Di Bartolomeo, L. Somma, et al. Doxifluridine in colorectal cancer patients resistant to 5-fluorouracil (5-FU) containing regimens. *Eur J Cancer* **1997**, 33 (4), 687–690.
21. R.D. Armstrong, E. Cadman. 5'-Deoxy-5-fluorouridine selective toxicity for human tumor cells compared to human bone marrow. *Cancer Res* **1983**, 43 (6), 2525–2528.
22. P. Alberto, B. Mermillod, G. Germano, et al. A randomized comparison of doxifluridine and fluorouracil in colorectal carcinoma. *Eur J Cancer Clin Oncol* **1988**, 24 (3), 559–563.
23. H. Hur, Y. Xuan, Y.B. Kim, etal. Expression of pyruvate dehydrogenase kinase-1 in gastric cancer as a potential therapeutic target. *Int J Oncol* **2013**, 42 (1), 44–54.
24. P. Wińska, O. Karatsai, M. Staniszewska, et al. Synergistic Interactions of 5-Fluorouracil with Inhibitors of Protein Kinase CK2 Correlate with p38 MAPK Activation and FAK Inhibition in the Triple-Negative Breast Cancer Cell Line. *Int J Mol Sci* **2020**, 21 (17), 6234.
25. W.L. Jorgensen, D.S. Maxwell, J. Tirado-Rives. Development and Testing of the OPLS All-Atom Force Field on Conformational Energetics and Properties of Organic Liquids. *J Am Chem Soc* **1996**, 118 (45), 11225–11236.
26. R.A. Friesner, R.B. Murphy, M.P. Repasky, et al. Extra Precision Glide: Docking and Scoring Incorporating a Model of Hydrophobic Enclosure for Protein−Ligand Complexes. *J Med Chem* **2006**, 49 (21), 6177–6196.
27. T.A. Halgren, R.B. Murphy, R.A. Friesner, et al. Glide: A New Approach for Rapid, Accurate Docking and Scoring. 2. Enrichment Factors in Database Screening. *J Med Chem* **2004**, 47 (7), 1750–1759.
28. R.A. Friesner, J.L. Banks, R.B. Murphy, et al. Glide: A New Approach for Rapid, Accurate Docking and Scoring. 1. Method and Assessment of Docking Accuracy. *J Med Chem* **2004**, 47 (7), 1739–1749.
29. K.J. Bowers, F.D. Sacerdoti, J.K. Salmon, et al. Molecular dynamics---Scalable algorithms for molecular dynamics simulations on commodity clusters. In *Proceedings of the 2006 ACM/IEEE conference on Supercomputing - SC '06*; ACM Press, New York, New York, USA, **2006**; p 84.
30. M. Bergdorf, S. Baxter, C.A. Rendleman, D.E. Shaw. Benchmark Chemical Systems and Simulation Parameters; **2015**.
31. W.L. Jorgensen, J. Chandrasekhar, J.D. Madura, R.W. Impey, M.L. Klein. Comparison of simple potential functions for simulating liquid water. *J Chem Phys* **1983**, 79 (2), 926–935.
32. K. Kashyap, R. Kakkar. Pharmacophore-enabled virtual screening, molecular docking and molecular dynamics studies for identification of potent and selective histone deacetylase 8 inhibitors. *Comput Biol Med* **2020**, 123, 103850.
33. M. Kato, J. Li, J.L. Chuang, D.T. Chuang. Distinct Structural Mechanisms for Inhibition of Pyruvate Dehydrogenase Kinase Isoforms by AZD7545, Dichloroacetate, and Radicicol. *Structure* **2007**, 15 (8), 992–1004.
34. R. Kakkar, R. Arora, P. Gahlot, D. Gupta. An insight into pyruvate dehydrogenase kinase (PDHK) inhibition through pharmacophore modeling and QSAR studies. *J Comput Sci* **2014**, 5 (4), 558–567.
35. by G. Ibrahim, M.I. H, E.A. Ahwany H, et al. AZ12 Based Design of PDK2 Inhibitors by Rita Kakkar, Neeta Azad, Pragya Gahlot 163 International Review of Biophysical Chemistry (I.RE; **2012**; Vol. 3.
36. N. Azad, M. Bhandari, R. Kakkar. Discovery of some potent PDHK inhibitors using pharmacophore modeling, virtual screening and molecular docking studies. *Journal of Biochemistry and Molecular Biology Research* **2016**, 2 (1), 67–72.
37. A. Tiwari, V. Tiwari, S. Kumar, et al. Molecular Docking and Simulation Analysis of Cyclopeptides as Anticancer Agents. *Curr Drug ther* **2023**, 18 (3), 247–261.